Average kinetic energy of the superconducting state

Mauro M. Doria,[1] S. Salem-Sugui, Jr.,[1] I. G. de Oliveira,[2] L. Ghivelder,[1] and E. H. Brandt[3]
[1]*Instituto de Física, Universidade Federal do Rio de Janeiro, C.P. 68528, 21945-970, Rio de Janeiro RJ, Brazil*
[2]*Faculdade de Ciências Exatas e Tecnológicas, Universidade Iguaçu-UNIG, Nova Iguaçu, 26260-100 RJ, Brazil*
[3]*Max Planck Institute für Metallforschung, Intitut für Physik, D-70506 Stuttgart, Germany*
(Received 12 February 2001; published 28 March 2002)

Isothermal magnetization curves are plotted as the magnetization times the magnetic induction, $4\pi M\cdot B$, versus the applied field H. We show here that this curve is the average kinetic energy of the superconducting state versus the applied field, for type-II superconductors with a high Ginzburg-Landau parameter κ. The maximum of $4\pi M\cdot B$ occurs at a field H^*, directly related to the upper critical field H_{c2}, suggesting that $H_{c2}(T)$ may be extracted from such plots even in cases when it is too high for direct measurement. We obtain these plots both theoretically, from the Ginzburg-Landau theory, and experimentally, using a Niobium sample with $T_c=8.5$ K, and compare them.

DOI: 10.1103/PhysRevB.65.144509 PACS number(s): 74.25.Ha, 74.25.Bt, 74.25.Fy

I. INTRODUCTION

The average kinetic energy in classical physics is a useful quantity that helps to obtain important information about several many-body systems, such as the Sun, whose internal temperature can be estimated in this way.[1] In cases when the interaction among particles is only partly known, and the virial theorem applies, the total energy can be directly related to the average kinetic energy, and the average kinetic energy to the equipartition theorem, leading to the prediction of thermal properties of the classical system. In this paper we demonstrate, both theoretically and experimentally, that the average kinetic energy of the superconducting state can be directly read from isothermal magnetization curves, for superconductors such that the Ginzburg-Landau parameter κ is larger than a few units. Thus this average only involves the paired electrons that form the condensate.

It is often the case in physics that just expressing data in a different way is sufficient to bring a different insight into the problem under investigation. This is exactly the present situation and we claim here that an interesting insight is obtained if isothermal magnetization $(4\pi M)$ data are plotted differently, namely, as the product $4\pi M\cdot B$, where the magnetic induction is $B=H+4\pi M$ and H is the equilibrium applied field. In this paper we show that this new curve $4\pi M\cdot B$ directly determines the average kinetic energy for superconductors with $\kappa>\kappa_c$, with an accuracy of less than 1% for $\kappa_c\approx 3$.

A remarkable property of the product $4\pi M\cdot B$ is that it may have several local minima along the mixed state. This property follows from the fact that $4\pi M\cdot B$ vanishes at both critical fields, H_{c1} and H_{c2}. At H_{c1}, M reaches a minimum and B vanishes, whereas at H_{c2}, B is maximum and M vanishes. Since $4\pi M\cdot B$ vanishes at two fields, the two extremes of the mixed state, it must necessarily have an absolute minimum in between, and possibly several local minima. The connection between the average kinetic energy and the isothermal magnetization follows from the virial theorem for superconductivity,[2] which states that

$$\frac{\mathbf{H}\cdot\mathbf{B}}{4\pi}=F_{kin}+2F_{field}, \tag{1}$$

where F_{kin} and $F_{field}=\langle \mathbf{h}^2/8\pi\rangle$, are the average kinetic energy and the average magnetic energy, respectively. The local magnetic field inside the superconductor is $\mathbf{h}$ and $\langle\cdots\rangle$ represents an average value taken over the volume of the superconductor. This theorem has been discovered rather late for the Ginzburg-Landau (GL) theory and it has been proven very useful since then, because it avoids taking the derivative of the free energy for the determination of H. The theorem has been extended to the microscopic theory in the context of the quasiclassical Eilenberger theory.[3] There it was found that the above theorem holds for temperatures well below T_c and also in presence of nonmagnetic impurities. Thus one expects that even in presence of some types of pinning the above relationship still holds.

In this paper we obtain $4\pi M\cdot B$ curves both theoretically and experimentally for isotropic superconductors. We only discuss here examples such that the symmetry along the direction defined by the applied field turns the theoretical problem into a two-dimensional one. In this case the vector notation is no longer necessary and so, is dropped hereafter. The $4\pi M\cdot B$ theoretical curve is derived in three situations of the macroscopic GL theory. We obtain analytical expressions for it in the Abrikosov and the London limits. we also calculate this curve numerically, using the iterative scheme proposed by E. H. Brandt,[4] a very accurate method that gives the periodic solution of the GL theory for any field in the mixed state. Using the iterative method we show that for κ larger than a few units the curve $4\pi M\cdot B$ indeed gives the average kinetic energy. The absolute minimum of the new curve,

$$\left.\frac{d(4\pi M\cdot B)}{dH}\right|_{H^*}=0, \tag{2}$$

determines a critical field called H^*. A consequence of the connection established here is that this field determines the maximum average kinetic energy, and from this one obtains the maximum root-mean-square current density, $J_{max}\equiv\sqrt{\langle J^2\rangle}$. Thus using the present approach one obtains information about the maximum current density without the use of Bean's model. For this one needs the London expression

$F_{kin} \approx 2\pi\lambda^2\langle J^2\rangle/c^2$, where λ is the penetration depth. Actually at H^* the order parameter is not constant but we consider it as such, to obtain the order of magnititude of this maximum current density circulating in the superconducting state.

In this paper we also show that the ratio H^*/H_{c2} becomes κ independent for κ larger than a few units. This property can be useful because it suggests that H_{c2} can be determined at a lower field, namely H^*. Frequently the upper critical field of many compounds cannot be reached experimentally just because it falls beyond the capabilities of a given experimental setup.

The $4\pi M\cdot B$ experimental curves were obtained here using a Niobium sample with an approximately spherical shape, mass $m=0.6487g$, and critical temperature $T_c=8.5$ K with a transition width of $\Delta T\sim 0.3$ K. The sample was obtained in an arc-melt furnace from 99.9% purity Nb wire. X-ray diffraction done in this sample shows the expected metallic Nb phase. Isothermal magnetization data were always obtained starting from a zero-field cooled procedure and using a commercial Quantum Design PPMS extraction magnetometer facility.

Features and properties not visible in the traditional way of plotting magnetization curves are unveiled here by this $4\pi M\cdot B$ plot. Some of them are explained in this paper, but there are others, such as the multiminima structure in the irreversible region, that require further discussion not done here. In the reversible region, only one minimum remains and we find good agreement between theory and experiment. Close to T_c the experimental and theoretical $4\pi M\cdot B$ curves show good agreement and the experimental ratio H^*/H_{c2} is well predicted by the present theoretical models. Notice that the virial theorem, Eq. (1), holds for the microscopic theorem,[3] and for this reason the connection between the curve $4\pi M\cdot B$ and F_{kin} remains valid beyond the GL theoretical framework of this paper.

This paper is organized as follows. In Sec. II we show that the curve $4\pi M\cdot B$ gives the average kinetic energy of the superconducting state and derive this curve both analytically and numerically in different theoretical situations. The field H^* is calculated and its properties discussed here. In Sec. III the experimental $4\pi M\cdot B$ curves for the Nb sample are obtained, and the field H^* determined. The phase diagram of this Nb sample is obtained with the curve $H^*(T)$ included. Finally we draw conclusions in Sec. IV.

II. THEORY

Let us first obtain analytical expressions for the energy function $4\pi M\cdot B$ in two simple situations and determine there the critical field H^*. The lower and upper critical fields are given by $H_{c1}=(\Phi_0/4\pi\lambda^2)\ln\lambda/\xi$ and $H_{c2}=\Phi_0/2\pi\xi^2$, respectively, ξ is the coherence length, and $\kappa=\lambda/\xi$ the Ginzburg-Landau parameter. The first case investigated here is Abrikosov's theory which calculates the vortex lattice near H_{c2} in the framework of the GL free energy. There[5] the magnetic induction is given by

$$B=H-\frac{H_{c2}-H}{(2\kappa^2-1)\beta_A}, \tag{3}$$

where $\beta_A=\langle|\Delta|^4\rangle/\langle|\Delta|^2\rangle^2$ is a parameter determined from the vortex lattice symmetry, Δ being the wave function that describes the superconducting state. One obtains that

$$4\pi M\cdot B=-\frac{H_{c2}-H}{(2\kappa^2-1)\beta_A}\left(H-\frac{H_{c2}-H}{(2\kappa^2-1)\beta_A}\right) \tag{4}$$

is a parabola that vanishes at $H_{c2}/[1+(2\kappa^2-1)\beta_A]$ and at H_{c2}. Although Abrikosov's theory is valid only near H_{c2}, still, for $\kappa\gg\sqrt{2}/2$, the first vanishing field approaches $2/(1+2\beta_A)\Phi_0/4\pi\lambda^2$, which is of the same order of magnitude as the true H_{c1} field. The absolute minimum of $4\pi M\cdot B$ is achieved at the field

$$H^*=\frac{H_{c2}}{2}\left(\frac{2\beta_A\kappa^2-\beta_A+2}{2\beta_A\kappa^2-\beta_A+1}\right). \tag{5}$$

A simpler expression is obtained noting that β_A is very close to 1, which is true for the triangular lattice ($\beta_A=1.159\,595\,3\cdots$): $H^*\approx(H_{c2}/2)^*(1+1/\kappa^2)$. Thus for any superconductor with κ larger than a few units, this critical field is given by $H\approx 0.5H_{c2}$.

The second model is London theory, known to provide a good description of the superconducting state in the intermediate field region far away from the critical fields. This is a fairly good approximation as long as variations of the order parameter near the vortex cores can be ignored, and so, the order parameter can be considered constant all over the superconductor. In this region the magnetic induction is very well approximated by[5]

$$B=H-H_{c1}\frac{\ln(H_{c2}/B)}{\ln\kappa}. \tag{6}$$

Then the energy function becomes

$$4\pi M\cdot B=-BH_{c1}\frac{\ln(H_{c2}/B)}{\ln\kappa} \tag{7}$$

whose absolute minimum is at the field value

$$H^*=\frac{H_{c2}}{e}-\frac{H_{c1}}{\ln\kappa}. \tag{8}$$

Since $H_{c1}/H_{c2}=\ln\kappa/2\kappa^2$, notice, once more, that in case κ is larger than a few units the last term can be neglected, rendering $H^*\approx 0.37H_{c2}$.

The product $4\pi M\cdot B$ is related to the average kinetic energy of the condensate, without any approximation, through the virial theorem [Eq. (1)]:

$$4\pi M\cdot B=-F_{kin}/2-\langle(h-\langle h\rangle)^2\rangle, \tag{9}$$

is expressed here in reduced units, such that the thermodynamical fields and energies are scaled in the following way: $h\to h/\sqrt{2}H_c$, $H\to H/\sqrt{2}H_c$, and $F_{kin}\to F_{kin}/(H_c^2/4\pi)$, H_c being the thermodynamic field. The same scaling holds for the magnetic induction which is just the average local field, $B\equiv\langle h\rangle$. These reduced units are convenient because to re-

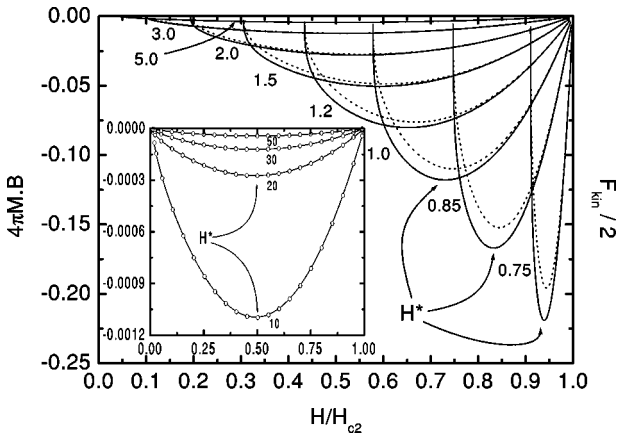

FIG. 1. Two theoretical curves, $4\pi M\cdot B$ (continuous) and $F_{kin}/2$ (dots), versus H are shown here for several κ, namely, 0.75, 0.85, 1.0, 1.2, 1.5, 2.0, 3.0, and 5.0. For higher κ, 10, 20, 30, and 50, the two curves, $4\pi M\cdot B$ (continuous) and $F_{kin}/2$ (points), are shown in the inset. The field H^*, the absolute minimum of the $4\pi M\cdot B$ curve, is suggested for a few curves, as examples. The inset clearly shows that for large κ $H^*/H_{c2}\approx 0.5$.

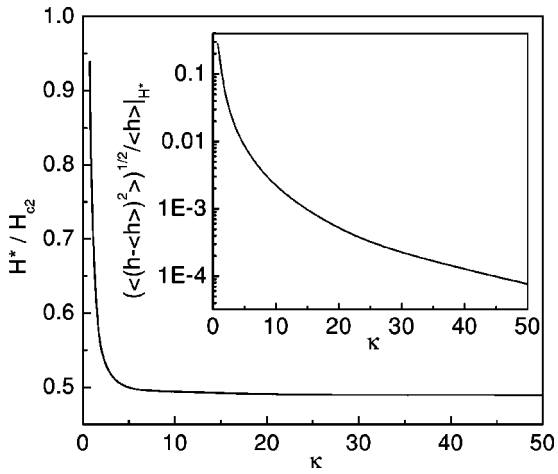

FIG. 2. The field H^*, the absolute minimum of the $4\pi M\cdot B$ curve, is plotted here as a function of κ. For κ larger than a few units the ratio H^*/H_{c2} approaches 0.5. The inset shows that the root-mean-square deviation of the local field vanishes for κ larger than a few units.

trieve the above quantities at any given temperature T from a single temperature-independent plot, it is enough to scale energies by $H_c(T)^2/4\pi$, and fields by $\sqrt{2}H_c(T)$.

To show that the function $4\pi M\cdot B$ yields the average kinetic energy F_{kin} is just a matter of determining how the mean-square deviation of the local field $\langle(h-\langle h\rangle)^2\rangle$ behaves as a function of κ. This is done here for the GL theory using the iterative method of E. H. Brandt.[4] This iterative procedure assumes an initial solution, from which one obtains very accurately, after a few iterative steps, the local magnetic field and the order parameter for any applied field in the mixed state. The $4\pi M\cdot B$ (continuous line) and F_{kin} (points) curves, obtained using this method, are shown in Fig. 1 for several κ, ranging from 0.75 to 50. The conclusion is that these two curves, $4\pi M\cdot B$ and $F_{kin}/2$, become very similar for large κ. The field H^* is obtained by determining the absolute minimum of the $4\pi M\cdot B$ curves in Fig. 1, and Fig. 2 summarizes these results as a H^*/H_{c2} vs κ plot.

The difference between $4\pi M\cdot B$ and $F_{kin}/2$ is best quantified, as function of κ, by two variance ratios introduced here and both computed at the field H^*. We compute $\langle(h-\langle h\rangle)^2\rangle/|4\pi M\cdot B|_{H^*}$ for a few points $[\kappa,\langle(h-\langle h\rangle)^2\rangle/|4\pi M\cdot B|_{H^*}]$: (0.75,0.11), (0.85,0.094), (1.0,0.072), (1.5,0.034), (2.0,0.020), (3.0,0.0088), (5.0,0.0032), $(10.0,7.83\times10^{-4})$, $(20.0,1.99\times10^{-4})$, $(30.0,8.8\times10^{-5})$, and $(50.0,3.2\times10^{-5})$. Notice that for $\kappa>3$ the two curves can be regarded as the same with an error of less than 1% in the neighborhood of H^*. This error is not uniform for all fields, being smaller near H_{c2} and larger near H_{c1}. In Fig. 2 one has that $H^*/H_{c2}=0.51$ for $\kappa=3.0$, and essentially, for $\kappa>3$, H^* is fairly well approximated by its limiting value of $0.5H_{c2}$. The inset of Fig. 2 shows the relative root-mean-square deviation of the local magnetic field, $[\langle(h-\langle h\rangle)^2\rangle]^{1/2}/\langle h\rangle|_{H^*}$, as a function of κ. Again we see a sharp drop of this quantity as κ increases. For instance, for $\kappa=3.0$, $[\langle(h-\langle h\rangle)^2\rangle]^{1/2}/\langle h\rangle|_{H^*}=0.0213$.

Analytical expressions for these two variances are obtained in the Abrikosov approximation which starts from the well-known Abrikosov relation between the local field and the order parameter,[8] $h=H-2\pi|\Delta|^2/\kappa$, in reduced units. From it one obtains an interesting expression that relates the variance to the magnetization: $\langle(h-\langle h\rangle)^2\rangle=(4\pi M)^2(\beta_A-1)$. From it one finds at the field H^*, given by Eq. (5), the following expressions:

$$\left.\frac{[\langle(h-\langle h\rangle)^2\rangle]^{1/2}}{\langle h\rangle}\right|_{H^*} = \left(\frac{\beta_A-1}{\beta_A}\,\frac{1}{4\beta_A\kappa^4-4(\beta_A-1)\kappa^2+(\beta_A-1)}\right)^{1/2} \tag{10}$$

and

$$\left.\frac{\langle(h-\langle h\rangle)^2\rangle}{|4\pi M\cdot B|}\right|_{H^*}=\frac{\beta_A-1}{2\beta_A\kappa^2+1-\beta_A}. \tag{11}$$

Both expressions display a $1/\kappa^2$ behavior for large κ. For the triangular lattice, one obtains that $[\langle(h-\langle h\rangle)^2\rangle]^{1/2}/\langle h\rangle|_{H^*}\approx 0.172\,256/\kappa^2$, and $\langle(h-\langle h\rangle)^2\rangle/|4\pi M\cdot B|_{H^*}\approx 0.068\,815/\kappa^2$, which agree quite well with the numerical method results. We conclude that the curve $4\pi M\cdot B$ can be obtained from the average kinetic energy for $\kappa>\kappa_c$, with a precision better than 1% for $\kappa_c\approx 3$. Next we study a niobium sample and obtain the curve $4\pi M\cdot B$ experimentally, starting from the isothermal magnetization curves.

III. EXPERIMENT

To exemplify the present ideas we have studied superconductor niobium, which along the years has been an important reference for the understanding of type-II superconducting properties.[6] The observation of the irreversibility line in pure

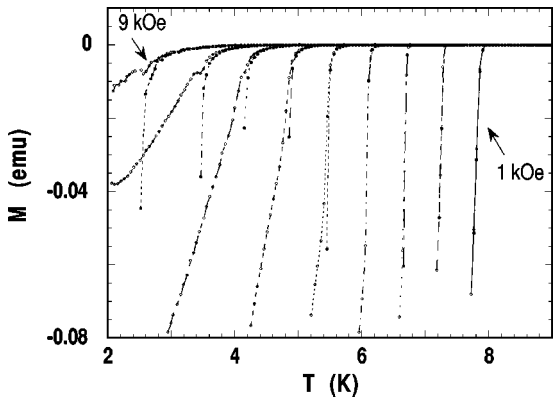

FIG. 3. The ZFC and FC magnetization versus temperature curves are shown here for several applied fields, ranging from 1.0 to 9.0 kOe every 1.0 kOe. Below 4.0 kOe the curves can be considered as reversible.

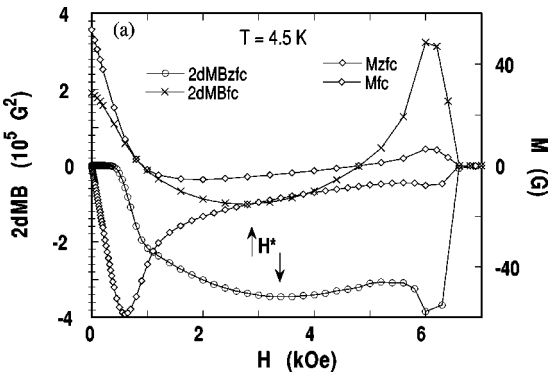

FIG. 5. A selected isothermal magnetization cycle is plotted here both in the traditional and in the new ways, for the temperature of 4.5 K. The field H^* is hardly noticeable whereas the peak effect is the absolute minimum of the $2dMB$ vs H curve.

Nb,[7] as observed in high-T_c superconductors,[9] has renewed the interest on this superconductor. Also, effects which are easier to study and understand in Nb, such as surface pinning,[10] vortex avalanches,[11] and peak effect,[12] has shed some light on the understanding of similar effects in high-T_c superconductors.

The sample has critical temperature below of pure Nb ($T_c = 9.2$ K), indicating that it contains nonmagnetic impurities. This causes no problem here; on the contrary, the impurities turn the compound into a more type-II superconductor, with a larger value of κ. Very pure Nb (Ref. 13) has $\kappa \approx 1.0$, whereas we find here $\kappa \approx 4$ for this sample, when comparing the present theory to the experiment.

Next we discuss our data as shown in the figures. The transition properties of this sample are seen in Fig. 3, which shows a rather small reversible temperature region. For fields below 4.0 kOe, the magnetization becomes essentially irreversible. Values of $H_{c2}(T)$ are extracted from this diagram following the standard linear extrapolation of the magnetization curve.

Figure 4 shows a total of nine isothermal magnetization cycles, 0.5 K apart from each other, for temperatures ranging from 3.5 to 8 K. Notice that in the neighborhood of zero applied field all the magnetization curves overlap forming one single temperature-independent line. The slope of this line defines the demagnetization factor. For finite-size samples the demagnetization factor must be included;[14] for a sphere this factor is 1/3 such that $B = H_{in} + 4\pi M/3$, where $H_{in} = H + 4\pi M/3$ is the internal field. Our sample is an ellipsoid with axis $2r_1 = 4.7$ mm and $2r_2 = 5.3$ mm, whose sphere with equivalent volume has radius 5.1 mm. We have experimentally determined the demagnetization of our sample using the following procedure. We assume that $B = H + 2dM$ where d is a factor to be determined from our data such that, in the Meissner phase, the magnetic induction must vanish. We find that, in this region, a linear extrapolation of the magnetization data for all $4\pi M$ vs H curves produces the same value of $2d = 4.16$, independent of temperature.

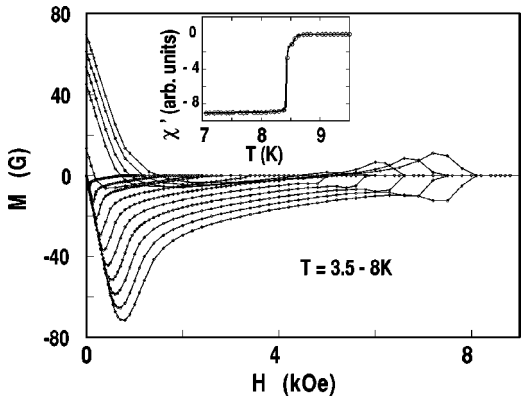

FIG. 4. Isothermal magnetization cycles measured in ascending (ZFC) and descending (FC) fields are shown, starting from 3.5 to 8 K every 0.5 K. The overlap of the inital part of the cycles into a single straight line defines the demagnetization factor of the sample.

Another important issue here is the removal of the background magnetization as a function of H for all temperatures. The construction of the curve $4\pi M \cdot B$ is only useful, e.g., to determine the critical field H^*, if all magnetic contributions that are not of superconducting origin are totally removed from the original isothermal M vs H data. For the Nb sample the following procedure was applied. The raw magnetization data display a linear nonzero positive slope as a function of H that goes beyond the H_{c2} field. This curve is universal and temperature independent. We subtract from the raw magnetization data at all temperatures this single linear curve M vs H. This is possible because the background magnetization is temperature independent, and just a single measurement of the paramagnetic background signal close or above T_c is enough to subtract the unwanted background for any temperature. It is well known that this source of magnetic signal is the Pauli paramagnetism of the normal electrons.

Selected isothermal curves $2dMB$ vs H are shown for three different temperatures, corresponding to $T = 4.5$,6, and 8 K (Figs. 5, 6, and 7, respectively). The basic features of the M vs H curves, such as the critical fields and the peak effect, are also present in the $2dMB$ vs H curves, although in a somewhat different way. However, the $2dMB$ shows a feature not noticed in the traditional M vs H plot, namely the

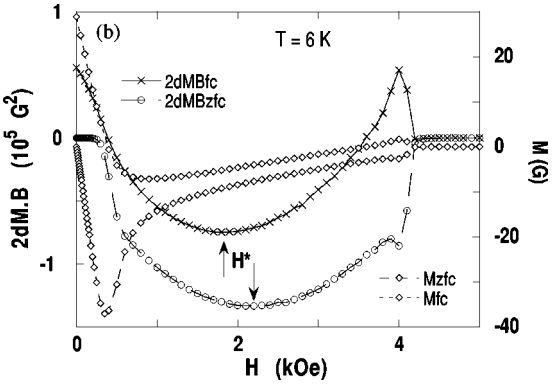

FIG. 6. A selected isothermal magnetization cycle is plotted here both in the traditional and in the new ways, for the temperature of 6.0 K. The field H^* is the absolute minimum, whereas the peak effect is just a local one, for the $2dMB$ vs H curve.

new minimum at H^*. For $T=4.5$ K the absolute minimum of the curve $2dMB$ occurs at $H=6.0$ kOe, a field associated with the peak effect. Still the H^* is observable there. However, for increasing temperature, $T=6$ K, H^* becomes the absolute minimum and the peak effect turns into a local minimum, in this case around 4 kOe. Finally at $T=8$ K only one minimum remains, H^*, and the peak effect is essentially absent. Notice that two H^* fields are defined, measured in ascending (zero-field-cooled, ZFC) and descending (field-cooled, FC) fields. The ZFC and FC H^* fields are separated by approximately 500 Oe for the $T=4.5$-K curve whereas for 8 K they become the same.

In Fig. 8 we compare the $\kappa=3,4$, and 5 theoretical and the $T=8.0$ K experimental curves obtained in this paper. All $2dMB$ data sets are normalized along the $2dMB$ axis to their maximum absolute values, achieved at H^*. Along the H axis, the theoretical curves are scaled by the inverse of their upper critical fields, such as in Fig. 1. However, for the experimental curve we adopted another normalization procedure, namely we scaled fields by 796.98 H due to the following reason. Our goal is to shift the $2dMB$ experimental curve along the H axis in search of the best theoretical fit, which we find to occur when experimental and theoretical

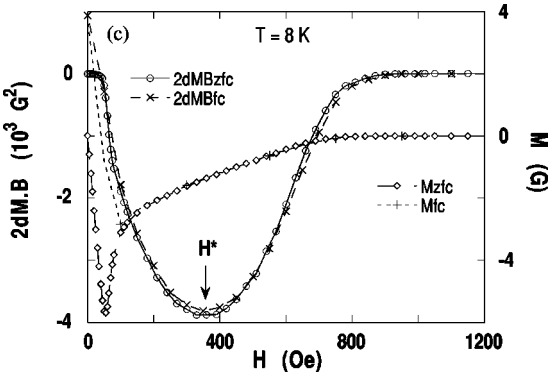

FIG. 7. A selected isothermal magnetization cycle is plotted here both in the traditional and in the new ways, for the temperature of 8.0 K. The field H^* is the absolute minimum of the $2dMB$ vs H curve, which is essentially totally reversible.

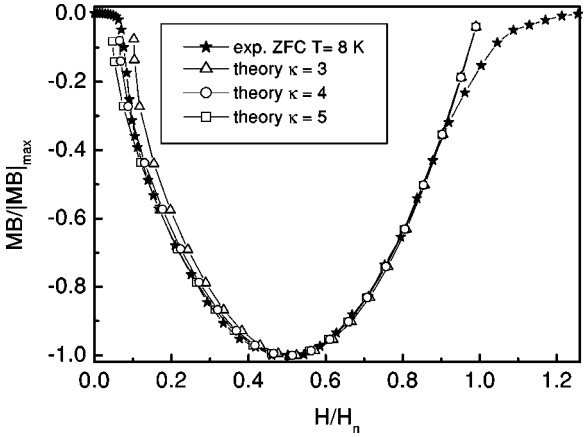

FIG. 8. This plot shows the theoretical curves ($\kappa=3$, 4, and 5) and that, among them, the $\kappa=4$ curve provides the best fitting to the $T=8-$K experimental curve. All four curves were normalized to their maximum absoulte value. Along the H axis the three theoretical curves were scaled by their H_{c2}, and the experimental curve was scaled such that its H^* field is 0.46 away from the theoretical normalized H_{c2} field.

H^* fields coincide. The experimental absolute maximum of $|2dMB|$ is reached at $H^*=329.81$ Oe. Next we apply the scale transformation $\alpha H/329.81$ and search for α that gives the best agreement with the theoretical curves. This happens at $\alpha=0.46$, very close to the theoretical expected ratio of $\alpha=H^*/H_{c2}\approx 0.5$ of the theoretical curve, described in Fig. 2. Notice that the three theoretical curves coincide near H_{c2}, as they should, because of the normalization, but not near H_{c1}. From this figure we conclude that the theoretical $\kappa=4$ curve provides the best fitting to the experimental data. It is worth mentioning that this value of κ agrees with its experimental estimate derived from the ratio of the critical fields. H_{c2}/H_{c1}.

Figure 9 presents the phase diagram, obtained from the values of H_{c2} that follows from the curves of Fig. 3. Also plotted in this figure are the values of H^* found in the increasing and decreasing field branches of plots, such as shown in Figs. 5–7.

We find a quite perfect match between the experimental values of H^* and $H_{c2}(T)$ with the expression obtained from the theories previously discussed. Thus for this Nb sample

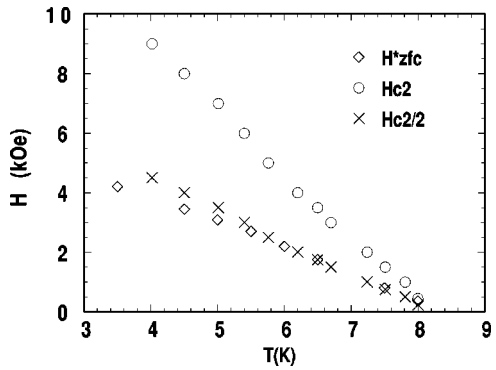

FIG. 9. The phase diagram of the Nb sample, containing its several critical fields, is shown here.

we find that the curve $H_{c2}/2$ fits fairly well the experimental H^* curve.

We estimate the maximum root-mean-square average current J_m for $T=8$ K. First one must obtain the London penetration depth from the lower critical field for this temperature: $H_{c1}\approx 18$ Oe. We obtain that $\lambda\approx 0.36\ \mu$m and taking that the maximum of $|2dM\cdot B|$ is reached at 3.88×10^3 G^2, it follows that $J_m\approx 4.2\times 10^5$ A cm^{-2}. Notice that this maximum mean-square average current density is being obtained in the *reversible* regime.

In summary we find here that this $4\pi M\cdot B$ curve naturally enhances many aspects of traditional $4\pi M$ vs H plots, such as the peak effect, the first entry field (H_{c1}), which is also much more clearly resolved in this kind of plot. Obviously the theories considered in the previous section do not describe the many features of the experimental curves $2dMB$ vs H, especially when irreversible processes are present. This is expected because those theories do not take into account pinning effects. When pinning effects become small and there is reversibility in the magnetization, we found agreement between theory and experiment. It is always possible to cast isothermal magnetic data as a $4\pi M\cdot B$ curve, but the question is whether the present connection between the $4\pi M\cdot B$ curve and F_{kin} still holds when irreversible effects are present, such as the peak effect. We believe that this connection indeed remains valid in the irreversible region in some large κ limit. Obviously this connection should always be regarded approximately and corrections are expected due to pinning. We believe that these corrections should be small, based on the fact that the virial theorem gets little or no modification at all[3] when some types of defects[2,15,16] are present. For temperatures close to T_c, where irreversible effects become small, we found that the present ideas hold and the average kinetic energy interpretation of the curve $4\pi M\cdot B$ is applicable.

IV. CONCLUSIONS

In conclusion the present proposal of casting isothermal magnetization data as the product of the magnetization times the magnetic induction is useful because it directly gives the average kinetic energy of the superconducting state for any applied field. We have studied here this curve both theoretically and experimentally. The field of maximum average kinetic energy in the condensate is just the minimum point of the new curve. From this field we estimate the maximum mean-square average current density. We show using the Ginzburg-Landau theory that this field value is half the upper critical field value for large κ superconductors. Thus its experimental determination can help us to understand properties of the upper critical field which often falls beyond the experimental capabilities of a given equipment. We found analytical expressions for this curve in two special limits of the Ginzburg-Landau theory, namely the Abrikosov and the London limits. In the general situation we have obtained this curve numerically for several values of the Ginzburg-Landau constant, using an efficient iterative method[4] to solve the Ginzburg-Landau theory. We find that for a Ginzburg-Landau constant larger than a few units the mean-square deviation of the local magnetic field becomes extremely small. Only for such parameter values does the product magnetization times the magnetic induction give the average kinetic energy. In summary we find the present proposal of plotting the isothermal magnetization useful because it provides interesting insight into the properties of the mixed state.

ACKNOWLEDGMENTS

This work was supported by a collaboration agreement DAAD-CNPq and in part by FAPERJ and CAPES.

[1] C. Kittel, W.D. Knight, and M.A. Ruderman, *Mechanics, Berkeley Physics Course* (McGraw-Hill, New York, 1965).
[2] M.M. Doria, J.E. Gubernatis, and D. Rainer, Phys. Rev. B **39**, 9573 (1989).
[3] U. Klein and B. Pöttinger, Phys. Rev. B **44**, 7704 (1991).
[4] E.H. Brandt, Phys. Rev. Lett. **78**, 2208 (1997).
[5] M. Tinkham, *Introduction to Superconductivity* (McGraw-Hill, New York, 1975).
[6] X.S. Ling *et al.*, Phys. Rev. Lett. **86**, 712 (2001).
[7] R.M. Suenaga, A.K. Ghosh, Y. Xu, and D.O. Welsh, Phys. Rev. Lett. **66**, 1777 (1991).
[8] E.H. Brandt, Rep. Prog. Phys. **58**, 1465 (1995).
[9] G. Blatter, *et al.*, Rev. Mod. Phys. **66**, 1125 (1994).
[10] P.K. Mishra, G. Ravikumar, V.C. Sahni, M.R. Koblischka, and A.K. Grover, Physica C **269**, 71 (1996).
[11] E.R. Nowak, O.W. Taylor, Li. Liu, H.M. Jaeger, and T.I. Selinder, Phys. Rev. B **55**, 11 702 (1997).
[12] Y. Kopelevich and P. Esquinazi, J. Low Temp. Phys. **113**, 1 (1998).
[13] D.K. Finnemore, T.F. Stromberg, and C.A. Swenson, Phys. Rev. B **149**, 231 (1966).
[14] J.D. Jackson, *Classical Electrodynamics*, 2nd ed. (John Wiley & Sons, Inc., New York, 1975).
[15] Mauro M. Doria, and Sarah C.B. de Andrade Phys. Rev. B **60**, 13 164 (1999).
[16] Mauro M. Doria and Sarah C.B. de Andrade, Phys. Rev. B **53**, 3440 (1996).